RESIDUAL-BASED VARIATIONAL MULTISCALE SIMULATION OF EROSION USING `libMesh`

Malú Grave

malugrave@nacad.ufrj.br

José J. Camata

camata@nacad.ufrj.br

Alvaro L.G.A. Coutinho

alvaro@nacad.ufrj.br

High Performance Computing Center, Federal University of Rio de Janeiro

P.O. Box 68506, 21945-970, RJ, Rio de Janeiro, Brazil

Abstract. *Sediment transport induced by fluid flows is a field of great interest in modern hydraulic science due to its great importance in engineering applications. Flood control, canals for irrigation, navigation and other projects are strongly affected by moving sediments. Depending on the intensity of the flow, erosion can appear at the bottom, for example. It occurs when the sediment bed changes by losing its mass as a consequence of sediment entrainment into suspension. Once out of the bottom, the finer sediments can be maintained in suspension by turbulence or deposited due to the gravitational acceleration. These phenomena are implemented as numerical models in* `libMesh`*, an open finite element library that provides a framework for numerical simulations in multiphysics. Here, the mathematical model results from the incompressible Navier-Stokes equation combined with an advection-diffusion transport equation for suspended sediments. The Navier-Stokes equation is treated with the residual-based variational multiscale finite element formulation while the advection-diffusion transport equation uses a stabilized method and a discontinuity capturing formulation. An empirical model is used to represent the entrainment rate. Special boundary conditions at the bottom are introduced to take into account sediments entrainment, as well as deposition. Two well-documented test cases where experimental data are available are used to validate the model employed in the present study. Results are analyzed and discussed.*

Keywords: *Computational fluid dynamics, Finite Element, Sediment transport*

1 INTRODUCTION

The calculation of sediment transport induced by fluid flows is one of the most important tasks in hydraulic science and related areas. However, the prediction of this phenomenon is still very difficult due to its complexity. Some calculations depend on empirical formulations as the entrainment rate, which is the rate that sediments come into suspension due the flow stress at the bottom. Garcia and Parker (1991) reviewed entrainment rate models such as Einstein (1950), Engelund and Fredsøe (1976) and Van Rijn (1984). They concluded that Van Rijn's model performs very well against the existing data and it will be the model adopted in this work.

Not only the entrainment rate is important but also the deposition rate of sediments. It is known that the formation of topographical features can occur as a result of the depositional and erosional nature of gravity currents interacting with the bottom. In numerical simulations, these phenomena are modelled applying proper boundary conditions. Several numerical approaches have been used to model suspended sediment transport. Lin and Falconer (1996) developed a model applying a hybrid finite difference method combined with the finite volume method for predicting suspended sediment concentrations. Wu *et al.* (2000) developed a 3D numerical model with a finite-volume method on an adaptive, non-staggered grid, where the flow was calculated by solving the full Reynolds-averaged Navier-Stokes equations with the $k-\epsilon$ turbulence model. Liang *et al.* (2005) developed a 2D model using finite difference method in a general curvilinear coordinate system. They have examined the performance of two turbulence models, the standard $k-\epsilon$ and Smagorinsky subgrid scale model, on modelling time dependent scour processes. Qureshi and Baloch (2013) developed a 2D finite element model using an innovative non-dimensional parameter called diffusion Reynolds number, which is a controlling parameter for a stable and accurate solution of suspended sediment transport.

All mentioned authors have validated their algorithms against two well-documented test cases where experimental data are available. Their computed sediment concentration profiles were in close agreement with laboratory observations from Van Rijn (1986) and Wang and Ribberink (1986).

The aim of this work is to implement a model that can reproduce sediment transport as well. Therefore, these phenomena are implemented as numerical models in `libMesh`, an open-source library that provides a platform for parallel, adaptive, multiphysics finite element simulations (Kirk *et al.*, 2006). The Navier-Stokes equations are treated with the residual-based variational multiscale finite element formulation (RB-VMS) while an advection-diffusion equation representing particle concentration is solved using a stabilized method with discontinuity capturing formulation. Sedimentation effects are modelled by considering the settling velocity of the grains. The predictions also showed good agreement with the measurements from Van Rijn (1986) and Wang and Ribberink (1986).

The remainder of this work is organized as follows. In the next section, we present the mathematical setting for the numerical simulation of the flow and the corresponding RB-VMS finite element formulation. After that, we show the sediment transport governing equations, sediment boundary conditions and the corresponding finite element formulation. We then show two numerical examples. One reproduces the net entrainment of sediment from a loose channel bed and the other deals with the net deposition of sediments. The paper ends with a summary of our main findings.

2 FLUID FLOW MODEL

This section establishes the mathematical setting for the numerical simulation of fluid flows.

2.1 Governing equations

The Navier-Stokes equations lead to the following nonlinear mathematical problem to be solved: Let us consider the spatial domain in which the flow takes place along the interval $[0, t_f]$ given by $\Omega \subset R^{nsd}$, where nsd is the number of space dimensions. Let Γ denote the boundary of Ω. Find the pressure p (divided by the constant density) and the velocity $\mathbf{u}$ satisfying the following equations:

$$\nabla \cdot \mathbf{u} = 0 \text{ on } \Omega \times [0, t_f] \tag{1}$$

$$\frac{\partial \mathbf{u}}{\partial t} + \mathbf{u} \cdot \nabla \mathbf{u} - \nabla \cdot \sigma = \mathbf{f} \text{ on } \Omega \times [0, t_f] \tag{2}$$

with $\mathbf{f}$ being the body force vector per unity density and σ the stress tensor given as

$$\sigma(p, \mathbf{u}) = -p\mathbf{I} + \mathbf{T} \tag{3}$$

where $\mathbf{I}$ is the identity tensor and $\mathbf{T}$ is the deviatoric stress tensor,

$$\mathbf{T} = 2\nu\epsilon(\mathbf{u}) \tag{4}$$

In Eq. (4) ν is the kinematic viscosity and $\epsilon(\mathbf{u})$ is the strain rate tensor defined as

$$\epsilon(\mathbf{u}) = \frac{1}{2}(\nabla \mathbf{u} + (\nabla \mathbf{u})^T) \tag{5}$$

Essential and natural boundary conditions for Eq. (1) are $\mathbf{u} = \mathbf{g}$ on Γ_g and $\mathbf{n} \cdot \sigma = \mathbf{h}$ on Γ_h, where Γ_g and Γ_h are subsets of the domain boundary Γ. Functions $\mathbf{g}$ and $\mathbf{h}$ are given and $\mathbf{n}$ is the unit outward normal vector of Γ. A divergence-free velocity field $\mathbf{u_0}(\mathbf{x})$ is the initial condition.

2.2 Residual-based variational multiscale formulation

The Navier-Stokes equations along with proper boundary and initial conditions contain all information necessary to model fluid flows, including turbulent effects. It is possible to approximate them numerically using a computational grid fine enough to represent all relevant scales of the studied problem. But, the computational effort tends to limit the application of this method only to low Reynolds numbers. Thus direct numerical simulation (DNS) is still a challenge, particularly at high Reynolds numbers.

An alternative approach to DNS consists on Large Eddy simulations (LES). In this method, only large flow structures are solved, while the smaller ones, called subgrid components, are modeled (Sagaut *et al.*, 2006). Inspired by LES models, the variational multiscale methods (VMS) were introduced by Hughes (1995) and Hughes *et al.* (1998) as a general technique to model the subgrid scales in the numerical solution of partial differential equations. Hughes *et al.* (1998) also showed that stabilized methods could be derived from VMS, particularly for

solving the incompressible Navier-Stokes equations. Stabilization is needed to prevent spurious oscillations in convection-dominated flows when under-resolved meshes are employed, and also to prevent undesired pressure oscillations when equal-order interpolations for velocity and pressure are used.

The VMS methods define large scales by projection into appropriate function spaces and they are based on the variational formulation of the model problem. Compared to classical LES based on filtering, the VMS approach does not face difficulties associated to inhomogeneous non-commutative filters in wallbounded flows, and as consequence, it is mathematically consistent also in the presence of boundaries. Therefore the boundary conditions are incorporated into the mathematical analysis in a natural way (Ahmed *et al.*, 2017).

These methods applied to the simulation of turbulent flows are well-established models and they have experienced a fast development. The residual-based variational multiscale finite element formulation (RB-VMS) has emerged as an important numerical and theoretical framework for general multiscale problems in computational mechanics. This approach was introduced by Calo (2004) and it has been applied successfully to a number of problems, with several discretization methods. The RB-VMS method does not include an eddy viscosity, which appears as the numerical diffusion inherent to the model. Thus, it does not need any modeling of the subgrid scales by statistical theories of turbulence. The subgrid components are modeled in terms of the residual of the large scales, and they are introduced in the resolved scale equations. See Hughes *et al.* (2004) and Rasthofer and Gravemeier (2017) for detailed reviews.

For the present problem, we assume that the primitive variables are decomposed in two fields:

$$\mathbf{u} = \mathbf{u}^h + \mathbf{u}' \tag{6}$$

$$p = p^h + p' \tag{7}$$

where $(\mathbf{u^h}, p^h)$ are the large scale component of the solution (resolved one), whereas $(\mathbf{u}', p')$ are the subgrid complement (unresolved one). We would like to insert the previous splitting of scales in a standard variational Galerkin formulation built upon Eq. (1) and (2). For that, we assume the following weight space $S_{\mathbf{u}}$ and S_p for velocity and pressure respectively, along with their trial spaces counterparts $V_{\mathbf{u}}$ and V_p, and the weak formulation is described by: find $\mathbf{u} \in S_{\mathbf{u}}$ and $p \in S_p$ such that $\forall \mathbf{w} \in V_{\mathbf{u}}$ and $\forall q \in V_p$,

$$\begin{aligned}\left(\frac{\partial \mathbf{u}}{\partial t}, \mathbf{w}\right)_\Omega + (\mathbf{u}\cdot\nabla\mathbf{u}, \mathbf{w})_\Omega + (\sigma(p,\mathbf{u}), \epsilon(\mathbf{w}))_\Omega + \\ (\nabla\cdot\,\mathbf{u}, q)_\Omega = (\mathbf{f}, \mathbf{w})_\Omega + (\mathbf{h}, \mathbf{w})_{\Gamma_h}\end{aligned} \tag{8}$$

where $(.,.)_\Omega = \int_\Omega (.,.) d\Omega$ is the standard scalar product in $L^2(\Omega)$.

To come up with a feasible numerical scheme, some simplifications are introduced. We will admit the static hypothesis, such that the fine scales are algebraically related to the residuals of the governing equations. The time derivatives of the fine scales are supposed to vanish (rendering the denomination static fine scales), and the spatial derivatives in the fine scales equations are approximated through algebraic operators (much inspired on stabilized FEM) leading to the following set of fine scales equations:

$$\mathbf{u}' = \tau_m \mathbf{R_m} \tag{9}$$

$$p' = \tau_c R_c \tag{10}$$

where τ_c and τ_m are stabilization parameters given by the standard expressions of stabilized methods:

$$\tau_m = \left(\frac{4}{\Delta t^2} + \mathbf{u}^h \cdot \mathbf{G}\mathbf{u}^h + \nu^2 \mathbf{G}{:}\mathbf{G} \right)^{-\frac{1}{2}} \tag{11}$$

$$\tau_c = (\mathbf{g} \cdot \tau_m \mathbf{g})^{-1} \tag{12}$$

with $\mathbf{G}$ a second rank metric tensor,

$$\mathbf{G} = \frac{\partial \xi}{\partial \mathbf{x}}^T \frac{\partial \xi}{\partial \mathbf{x}} \tag{13}$$

and $\mathbf{g}$ a vector obtained from the column sums of $\frac{\partial \xi}{\partial \mathbf{x}}$,

$$\mathbf{g} = \{g_i\} \tag{14}$$

$$g_i = \sum_{j=1}^{d} \left(\frac{\partial \xi}{\partial \mathbf{x}} \right)_{ji} \tag{15}$$

The residuals for the continuity and momentum equations are respectively:

$$\mathbf{R_m} = \frac{\partial \mathbf{u}^h}{\partial t} + (\mathbf{u}^h - \mathbf{u}') \cdot \nabla \mathbf{u}^h + \nabla p^h - \nu \Delta \mathbf{u}^h - \mathbf{f} \tag{16}$$

$$R_c = \nabla \cdot \mathbf{u}^h \tag{17}$$

We now plug Eq. (6) and (9) to (17) into Eq. (8) and, after substituting and rearranging terms, the resulting equation representing the finite element problem to be solved is given by

$$\begin{aligned} &\left(\frac{\partial \mathbf{u}^h}{\partial t}, \mathbf{w}^h \right)_\Omega + \left((\mathbf{u}^h - \mathbf{u}') \cdot \nabla \mathbf{u}^h, \mathbf{w}^h \right)_\Omega + \left(\sigma(p^h, \mathbf{u}^h), \epsilon(\mathbf{w}^h) \right)_\Omega \\ &+ \left(\nabla \cdot \mathbf{u}^h, q^h \right)_\Omega + \left(\mathbf{u}', \mathbf{u}^h \cdot \nabla \mathbf{w}^h + \nabla q^h \right)_\Omega + \left(\tau_c \nabla \cdot \mathbf{u}^h, \nabla \cdot \mathbf{w}^h \right)_\Omega \\ &- \left(\mathbf{u}', \mathbf{u}' \cdot \mathbf{w}^h \right)_\Omega = \left(\mathbf{f}, \mathbf{w}^h \right)_\Omega + \left(\mathbf{h}, \mathbf{w}^h \right)_{\Gamma_h} \end{aligned} \tag{18}$$

3 SEDIMENT TRANSPORT MODEL

This section establishes the mathematical setting for the numerical simulation of sediment transport in fluid flows.

3.1 Governing equations

The sediment transport can be divided into two phenomena: suspended load and bed-load transport. The suspended load consists of the finer sediment maintained in suspension by turbulence, whereas, bed-load transport consists of coarse particles transported along the bed. In this work, the bed-load transport is not approached, but it is important to remind that it exists.

When the shear rate at the bottom is strong enough, sediments can entrain into suspension. The grains are moved out the bed-load zone and once out of the bottom, the finer sediments start to be governed by the suspended load equations. Furthermore, the suspended grains also can be deposited due to the gravitational acceleration and its settling velocity.

Suspended load. The governing equation for the suspended load is an advection-diffusion equation. By assuming a dilute suspension of small particles, we can neglect particle inertia and any particle-particle interaction. Consequently, the particles are driven by the fluid motion, with a settling velocity, u_s, which can be estimated by experiments or analytically and acts in the direction of gravity. Equation (19) presents the Stokes settling velocity:

$$u_s = \frac{d_{50}^2(\rho_s - \rho)g}{18\mu} \tag{19}$$

where d_{50} is the mean diameter of the sediment grain, ρ is the fluid density, ρ_s is the particle density, g is the gravitational acceleration and μ is the fluid viscosity.

Thus, the particles transport is governed by the following equation:

$$\frac{\partial c}{\partial t} + (\mathbf{u} + u_s \mathbf{e^g}) \cdot \nabla c = \nabla \cdot (\epsilon_s \nabla c) \text{ in } \Omega \times [0, t_f] \tag{20}$$

in which ϵ_s is the sediment diffusivity. The sediment diffusivity is related to the eddy viscosity ν_t by the turbulent Schmidt number Sc being $\epsilon_s = \nu_t / Sc$.

Assuming that the velocity follows the logarithmic law in the vertical direction, it is possible to derive a parabolic eddy viscosity distribution:

$$\nu_t = \kappa u_* y \left(1 - \frac{y}{H}\right) \tag{21}$$

where κ is the von Karman constant (0.42), H is the water depth, u_* is the bed-shear velocity and y is the vertical coordinate.

Entrainment and deposition rate. The entrainment rate needs an empirical model and, in this work, the model of Van Rijn (1984) is used. The entrainment rate is given by

$$E = C_{ae} u_s \tag{22}$$

where

$$C_{ae} = 0.015 \frac{d_{50}}{a} \frac{T^{1.5}}{d_*^{0.3}} \tag{23}$$

$$T = \frac{(u'_* - u_{*c})}{u_{*c}} \tag{24}$$

$$d_* = d_{50} \left(\frac{gR}{\nu^2}\right)^{\frac{1}{3}} \tag{25}$$

$$u_{*c} = \sqrt{\frac{\tau_{bc}}{\rho}} \tag{26}$$

$$\tau_{bc} = \theta_c \rho g R d_{50} \tag{27}$$

$$\theta_c = \frac{0.3}{1 + 1.2d_{*,n}} + 0.055(1 - e^{-0.02d_*}) \tag{28}$$

$$u'_* = \frac{g^{0.5}}{C'}\bar{u} \tag{29}$$

$$C' = 18\log\left(\frac{12R_b}{3d_{90}}\right) \tag{30}$$

In equations (22) to (30), C_{ae} is the near-bed sediment concentration in volume under capacity (equilibrium) status, a is the reference level above the bed, T is the transport parameter, d_* is the dimensionless grain size, u'_* is the effective bed shear velocity related to grain friction, u_{*c} is the critical bed-shear velocity for initial motion of sediment, R is the submerged specific gravity of sediment $\left(R = \frac{\rho_s - \rho}{\rho}\right)$, θ_c is the critical Shields number given by Soulsby and Whitehouse (1997), $\bar{u}$ is the mean flow velocity, R_b is the hydraulic radius according to the method of Vanoni-Brooks (1957) and d_{90} is the grain size corresponding to 90% finer.

On the other hand, the deposition rate at the bed is straightforward:

$$D = u_s c_b \tag{31}$$

where c_b is the sediment concentration very near the bed.

3.2 Sediment boundary conditions

For the following test cases, the suspended sediment concentration c is set to be the quantity of sediment entering in the flow domain at the inlet ($c = c_{in}$ on Γ^c_{in}). At the outlet, zero gradient is applied for c. At the atmosphere boundary and for the rigid walls, the flux of sediment through these surfaces is zero. And at the sediment bed, the flux of sediment is equal to $E - D$.

The flux of suspended sediment $\mathbf{q_s}$ including convective and diffusive fluxes is defined as

$$\mathbf{q_s} = (\mathbf{u} + u_s\mathbf{e^g})c - \epsilon_s \nabla c \tag{32}$$

Then the condition for zero flux of suspended sediment through the wall is expressed as

$$\mathbf{q_s} \cdot \mathbf{n} = 0 \text{ on } \Gamma^c_h \tag{33}$$

At the solid walls the velocity $\mathbf{u}$ will be always 0 because of the no-slip condition and, assuming a horizontal plane, the normal in this boundary is (0,1). Therefore, the boundary condition at this surface can be simplified as

$$u_s c + \epsilon_s \frac{\partial c}{\partial y} = 0 \text{ on } \Gamma^c_h \tag{34}$$

The same expression is found in the atmosphere, where the surface is also considered horizontal and the normal is (0,-1).

At the sediment bed, the sediment flux is specified as the net upward normal flux

$$\mathbf{q_s} \cdot \mathbf{n} = E - D \text{ on } \Gamma^c_{sed} \tag{35}$$

where D is the deposition rate and E is the entrainment rate.

Assuming a horizontal plane without bed morphology changes and knowing that the deposition rate is evaluated multiplying the settling velocity by the concentration near the bed, the boundary condition can be simplified as

$$\epsilon_s \frac{\partial c}{\partial y} = E \text{ on } \Gamma^c_{sed} \tag{36}$$

and, when there is only deposition (zero entrainment rate), the boundary condition becomes

$$\epsilon_s \frac{\partial c}{\partial y} = 0 \text{ on } \Gamma^c_{sed} \tag{37}$$

with $\Gamma = \Gamma^c_{in} \cup \Gamma^c_h \cup \Gamma^c_{sed}$ and $\Gamma^c_{in} \cap \Gamma^c_h \cap \Gamma^c_{sed} = \varnothing$.

3.3 Finite element formulation

The finite element formulation of Eq. (20) can be expressed as follows: Find $c \in S_c$ such that $\forall w \in V_c$,

$$\begin{aligned} \left(\frac{\partial c^h}{\partial t}, w\right)_\Omega + \left((\mathbf{u}^h - \mathbf{u}' + u_s \mathbf{e}^{\mathbf{g}}) \cdot \nabla c^h, w\right)_\Omega + (\epsilon_s \nabla c^h, \nabla w)_\Omega + \\ u_s (\mathbf{e}^{\mathbf{g}} \cdot \mathbf{n})(c^h, w)_{\Gamma^c_h \cup \Gamma^c_{sed}} + \left(\tau_t (\mathbf{u}^h - \mathbf{u}' + u_s \mathbf{e}^g) \cdot \nabla w^h, R_t\right)_{\Omega_e} + \\ \left(\nabla w^h, \kappa_{dc} \nabla c^h\right)_{\Omega_e} = (E - D)(c^h, w)_{\Gamma^c_{sed}} \end{aligned} \tag{38}$$

where R_t is the residual of transport Eq. (20),

$$R_t = \frac{\partial c}{\partial t} + (\mathbf{u}^h - \mathbf{u}' + u_s \mathbf{e}^{\mathbf{g}}) \cdot \nabla c^h - \epsilon_s \Delta c^h \tag{39}$$

with S_c and V_c being weight and trial finite element functions.

The above formulation makes use of the stabilization parameter τ_t that is given by

$$\tau_t = \left(\frac{4}{\Delta t^2} + \mathbf{u}^h \cdot \mathbf{G} \mathbf{u}^h + \epsilon_s^2 \mathbf{G} : \mathbf{G}\right)^{-\frac{1}{2}} \tag{40}$$

We also added to the formulation a discontinuity-capturing term κ_{dc}, based on the $YZ\beta$ discontinuity-capturing operator (Bazilevs *et al.*, 2007), defined as

$$\kappa_{dc} = \left(\frac{h_e}{2}\right)^\beta |\bar{c}^{-1} R_t| \left(\sum_{i=1}^{2} \left|\bar{c}^{-1} \frac{\partial c^h}{\partial x_i}\right|\right)^{\beta/2-1} \tag{41}$$

The parameter β in Eq. (41) influences the smoothness of the layer (for smoother layers it is set to 1), h_e is the characteristic height and the parameter $\bar{c}$ is the reference concentration. Note that if $\beta = 1$ and the reference concentration $\bar{c} = 1$, the discontinuity-capturing term renders to the Consistent Approximated Upwind method (Galeão and do Carmo, 1988).

4 VALIDATION OF THE SUSPENDED SEDIMENT TRANSPORT MODEL

Two well-documented test cases where experimental data are available are used to validate the model employed in the present study. One involves the net entrainment of sediment from a loose channel bed and the other deals with the net deposition of sediment. These two test cases are important to validate the sediment boundary conditions implemented. The bed-load transport of sediments is not included in these cases and also the sediments are considered passive scalars to the flow, meaning that they are carried by the flow but they do not change its behavior.

These phenomena are implemented as numerical models in an open-source library called `libMesh` (Kirk *et al.*, 2006). The `libMesh` library is a C++ framework for the numerical simulation of partial differential equations on serial and parallel platforms. It allows the users focus on their specific physic problem without having to develop the additional complexities for parallel or adaptive mesh computing, which are already implemented in the source code.

4.1 Net entrainment test case

In the Van Rijn (1986) entrainment test case, a fully-developed flow with clear water is introduced over the sediment bed and the sediment concentration is measured after the equilibrium condition is reached (Fig. 1). The original test conditions are employed in the present validation. The flow is steady and uniform with a water depth of 0.25 m and a mean velocity $\bar{u}$ of 0.67 m/s. The median diameter is 0.23 mm, d_{90} is 0.32 mm and the corresponding settling velocity is set to be 0.022 m/s. The reference level above the bed is taken to be 0.005 m and the predicted friction velocity is 0.047 m/s. The Schmidt number (Sc) is defined as 1 and the eddy viscosity is taken according to Eq. (21). The numerical simulation is made in 2D with real

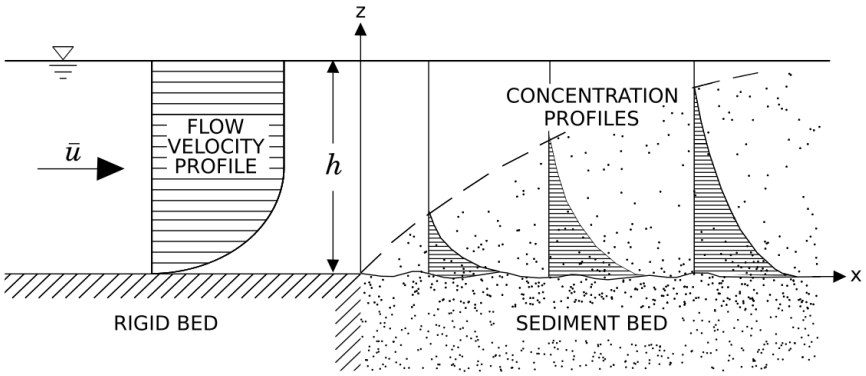

Figure 1: Net entrainment test case: Schematic definition of the problem

dimensions, $\Delta t = 0.0001\,\mathrm{s}$ and a mesh with 1640×40 quadrilateral elements. Figure 2 shows the flow boundary conditions which are: at the inlet, the profiles of the velocity are specified to be the fully developed values obtained from a separate calculation; for the rigid bed and the sediment bed, the no-slip condition is set; at atmosphere the slip condition is set; and zero velocity gradient is set at the outlet. The sediment boundary conditions are defined in section 3.2 with the sediment concentration c_{in} set to zero at the inlet which corresponds to clear water coming into the domain.

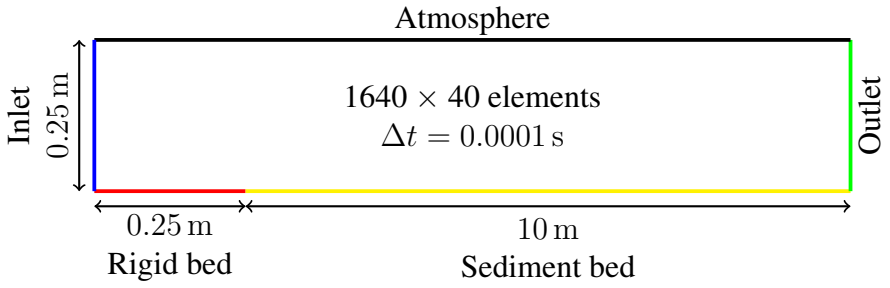

Figure 2: Net entrainment test case: boundary conditions

The initial conditions are zero sediment concentration in all domain and a fully-developed flow. Figure 3 illustrates the comparison of the computational and experimental sediment concentration distributions in four sections of the channel. It also shows results from Liang *et al.* (2005) and Wu *et al.* (2000). It can be seen that the simulation predicted the concentrations very well.

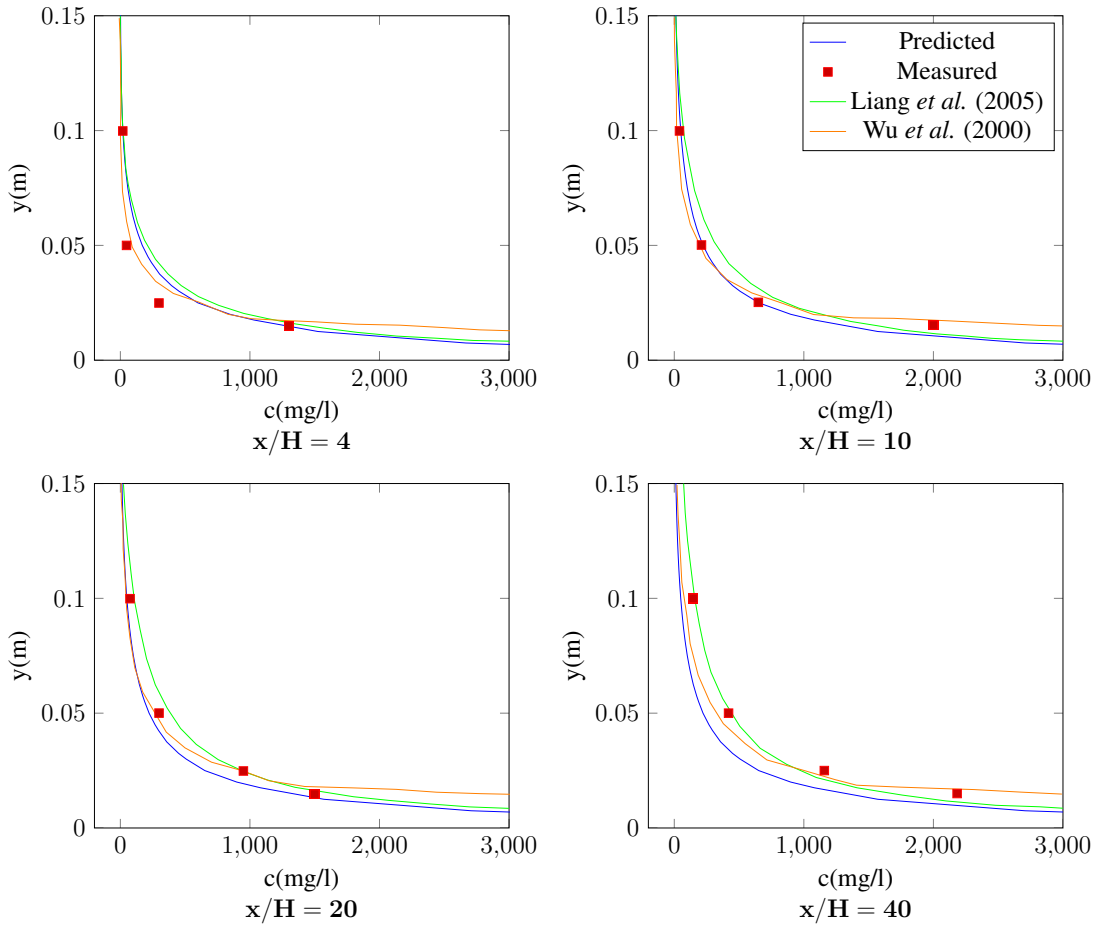

Figure 3: Net entrainment test case: comparison of the predicted (solid lines) and measured (squares) suspended sediment concentrations

4.2 Net deposition test case

Wang and Ribberink (1986) discharged sand into a flume whose bed is changed from rigid to perforated as shown in Fig. 4. Once the sediment fell to the bed, it was trapped into these compartments through the perforated plate and could hardly be entrained again. Hence, this case represents net deposition and the entrainment rate is considered zero at the bed. The flow is steady and uniform with a mean velocity $\bar{u}$ of $0.56\,\mathrm{m/s}$ and a water depth of $0.215\,\mathrm{m}$. The median sediment diameter is $0.095\,\mathrm{mm}$ and its fall velocity is $0.007\,\mathrm{m/s}$. The friction velocity is $0.034\,\mathrm{m/s}$, the Schmidt number (Sc) is taken to be 1 and the eddy viscosity is taken according to Eq. (21).

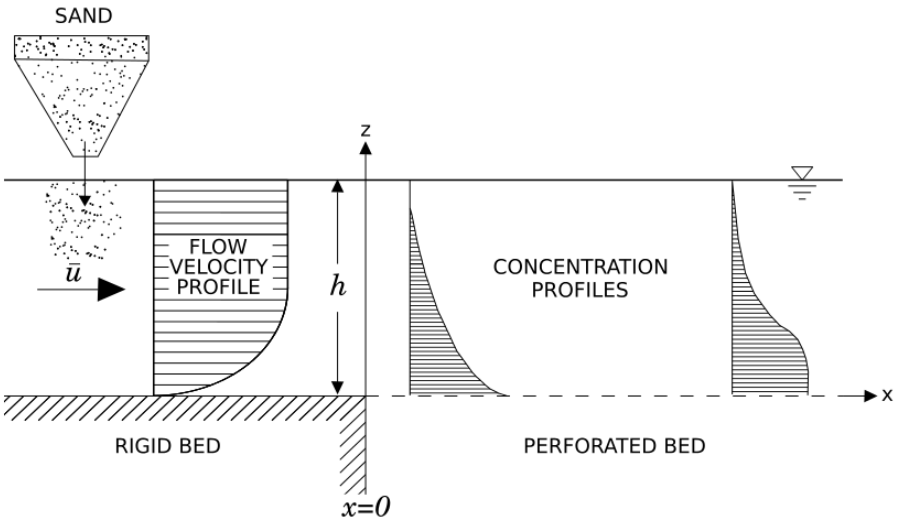

Figure 4: Net deposition test case: Schematic definition of the problem

The numerical simulation is made in 2D with real dimensions, $\Delta t = 0.0001\,\mathrm{s}$ and a mesh with 1600×22 quadrilateral elements. Figure 5 shows the flow boundary conditions which are: at the inlet, the profiles of the velocity are specified to be the fully developed values obtained from a separate calculation; at the perforated bed, the no-slip condition is set; at atmosphere, the slip condition is set; and zero velocity gradient is set at the outlet. The sediment boundary conditions are defined in section 3.2, but in this case, a measured sediment concentration profile is designated at the inlet and the entrainment rate at the perforated bed is 0, what means there is only deposition in this boundary.

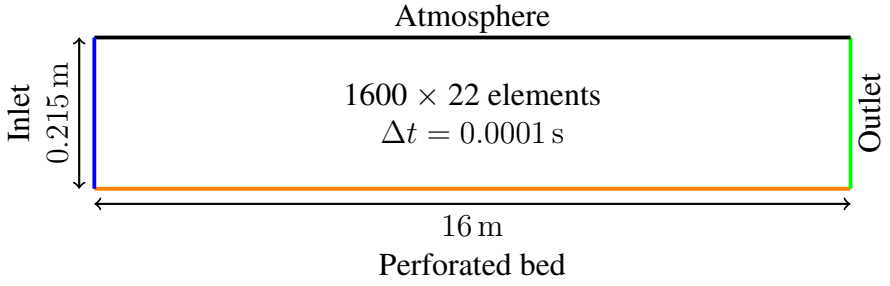

Figure 5: Net deposition test case: boundary conditions

The initial conditions are zero sediment concentration in all domain and a fully-developed flow whose velocities were calculated in a separated simulation. Figure 6 illustrates the comparison of the computational and experimental sediment concentration distributions in six sections of the channel. It also shows results from Liand *et al.* (2005) and Wu *et al.* (2000). It can be seen that once again the simulation predicted the concentrations very well.

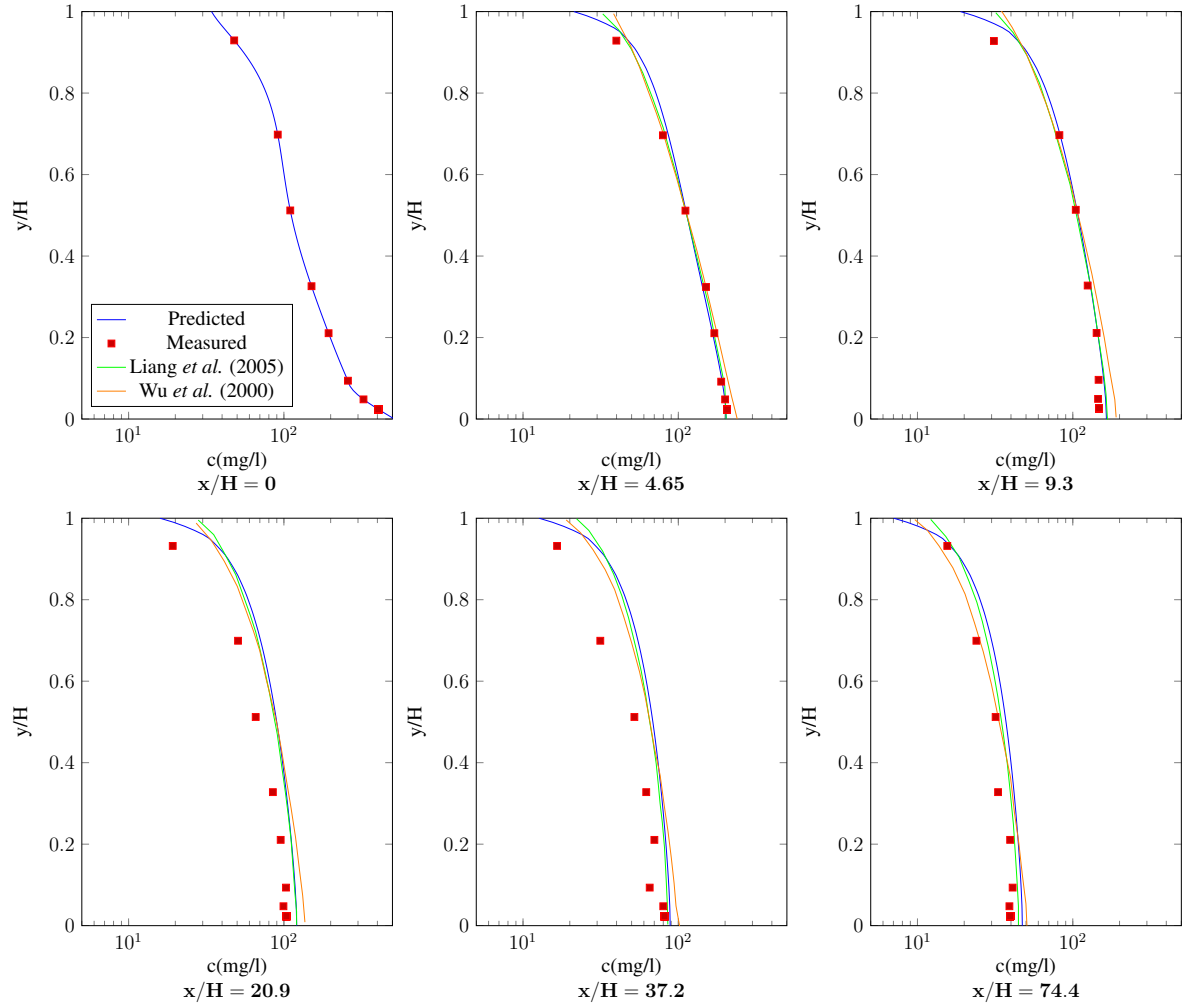

Figure 6: Net deposition test case: comparison of the predicted (solid lines) and measured (squares) suspended sediment concentrations

5 Conclusions

A 2D numerical model has been developed to predict the sediment concentration in fluid flows. The governing equations of sediment transport are approximated by a stabilized finite element formulation while the Navier-Stokes equation is treated with the RB-VMS method. The entrainment of sediments into suspension is modelled as a boundary condition using an empirical model to determine the entrainment rate. The concentration of suspended sediment is considered as a passive scalar.

The model was verified against two controlled physical experiments, one involving the net entrainment of sediment from a loose channel bed and the other dealing with the net deposition

of sediment. The predicted results showed good agreement with experimental data, showing that the suspended sediment transport model employed in this study works well for these cases.

As future work, the present model will be extended to incorporate bed-load transport and bed morphology changes in a way to represent all sediment transport phenomena.

ACKNOWLEDGEMENTS

The research has received funding from the European Union's Horizon 2020 Programme (2014-2020) under the HPC4E Project (www.hpc4e.eu), grant agreement n 689772, and from the Brazilian Ministry of Science, Technology, Innovation and Communications through Rede Nacional de Pesquisas (RNP). This work is also partially supported by CNPq, FAPERJ, Capes and Petrobras.

REFERENCES

Ahmed, N., Rebollo, T. C., John, V., & Rubino, S., 2017. A review of variational multiscale methods for the simulation of turbulent incompressible flows. *Archives of Computational Methods in Engineering*, vol. 24, n. 1, pp. 115-164.

Bazilevs, Y., Calo, V. M., Tezduyar, T. E., & Hughes, T. J. R., 2007. YZβ discontinuity capturing for advection-dominated processes with application to arterial drug delivery. *International Journal for Numerical Methods in Fluids*, vol. 54, n. 6-8, pp. 593-608.

Calo, V. M., 2004. *Residual-based multiscale turbulence modeling: finite volume simulations of bypass transition.* PhD thesis, Stanford University.

Einstein, H. A., 1950. *The bed-load function for sediment transportation in open channel flows*. Washington DC: US Department of Agriculture.

Engelund, F., & Fredøse, J., 1976. A sediment transport model for straight alluvial channels. *Hydrology Research*, vol. 7, n. 5, pp. 293-306.

Galeão, A. C., & do Carmo, E. G. D., 1988. A consistent approximate upwind Petrov-Galerkin method for convection-dominated problems. *Computer Methods in Applied Mechanics and Engineering*, vol. 68, n. 1, pp. 83-95.

Garcia, M., & Parker, G., 1991. Entrainment of bed sediment into suspension. *Journal of Hydraulic Engineering*, vol. 117, n. 4, pp. 414-435.

Hughes, T. J. R., 1995. Multiscale phenomena: Green's functions, the Dirichlet-to-Neumann formulation, subgrid scale models, bubbles and the origins of stabilized methods. *Computer Methods in Applied Mechanics and Engineering*, vol. 127, n. 1-4, pp. 387-401.

Hughes, T. J. R., Feijóo, G. R., Mazzei, L., & Quincy, J. B., 1998. The variational multiscale methods - a paradigm for computational mechanics. *Computer Methods in Applied Mechanics and Engineering*, vol. 166, n. 1-2, pp. 3-24.

Hughes, T. J. R., Scovazzi, G., & Franca, L. P., 2004. Multiscale and stabilized methods. In *Encyclopedia of Computational Mechanics*.

Kirk, B. S., Peterson, J. W., Stogner, R. H., & Carey, G. F., 2006. `libMesh`: a C++ library for parallel adaptive mesh refinement/coarsening simulations. *Journal Engineering with Computers*, vol. 22, n. 3-4, pp. 237-254.

Liang, D., Cheng, L., & Li, F., 2005. Numerical modeling of flow and scour below a pipeline in currents Part II. Scour simulation. *Journal of Hydraulic Research*, vol. 52, n. 1, pp. 43-62.

Lin, B., & Falconer, R. A., 1996. Numerical modelling of three-dimensional suspended sediment for estuarine and coastal waters. *Journal of Hydraulic Research*, vol. 34, n. 4, pp. 435-456.

Qureshi, A., & Baloch, A., 2013. Finite element simulation of sediment transport: Development, validation and application of model to Potho minor of Jamrao West Branch, Sindh, Pakistan. *Advances in Sediment Transport Research*.

Rasthofer, U., & Gravemeier, V., 2017. Recent Developments in Variational Multiscale Methods for Large-Eddy Simulation of Turbulent Flow. *Archives of Computational Methods in Engineering*, pp. 1-44.

Sagaut, P., Deck, S., & Terracol, M., 2006. *Multiscale and multiresolution approaches in turbulence*. Imperial College Press: London.

Soulsby, R. L., & Whitehouse, R. J. S., 1997. Threshold of sediment motion in coastal environments. In *Pacific Coasts and Ports' 97: Proceedings of the 13th Australasian Coastal and Ocean Engineering Conference and the 6th Australasian Port and Harbour Conference; Volume 1.*, Centre for Advanced Engineering, University of Canterbury, pp. 145-150.

Van Rijn, L. C., 1984. Sediment Transport, Part II: Suspended Load Transport. *Journal of Hydraulic Engineering., ASCE*, vol. 110, n. 11, pp. 1613-1641.

Van Rijn, L. C., 1986. Application of sediment pick-up functions. *Journal of Hydraulic Engineering, ASCE*, vol. 112, n. 9, pp. 867-874.

Vanoni, V. A., & Brooks, N. H., 1957. *Laboratory studies of the roughness and suspended load of alluvial streams*.

Wang, Z. B., & Ribberink, J. S., 1986. The validity of a depth-integrated model for suspended sediment transport. *Journal of Hydraulic Research*, vol. 24, n. 1, pp. 53-67.

Wu, W., Rodi, W., & Wenka, T., 2000. 3D numerical modeling of flow and sediment transport in open channels. *Journal of Hydraulic Engineering*, vol. 126, n. 1, pp. 4-15.